Manipulating the Solubility of Gold Nanoparticles Reversibly and Preparation of Water-Soluble Sphere Nanostructure through Micellar-like Solubilization

Yun Yang,[†,‡] Wei Wang,[‡] Jinru Li,[‡] Jin Mu,[*,†] and Huilin Rong[‡]

Department of Chemistry, East China University of Science and Technology, Shanghai 200237, and Key Laboratory of Colloid and Interface Sciences, Institute of Chemistry, Chinese Academy of Sciences, Beijing 100086, P.R. China

Received: February 11, 2006; In Final Form: July 6, 2006

On the basis of micellar solubilization, a strategy tuning the solubility of gold nanoparticles reversibly was developed. Hydrophobic gold nanoparticles stabilized by octadecylamine (ODA-gold) solubilized in the micellar-like core of poly(vinylpyrrolidone) (PVP) in water to form gold nanoparticles with protective multilayer induced by reduction of interfacial energy. Interestingly, upon redispersing in chloroform, the PVP micellar-like structure can break down and the ODA-gold can be released again. By changing the ratio of PVP/ODA, size-controllable hydrophilic spherical assembly can be prepared. On the basis of the observation of transmission electron microscopy (TEM) and Fourier transform infrared spectroscopy (FTIR), a reasonable mechanism is interpreted thermodynamically.

Introduction

It is well-known that many amphiphilic surfactants possess both a hydrophilic head and a hydrophobic tail which always render the surfactants soluble in water and organic solvent. In water or organic solvent, due to the minimum energy rule, these substances employ certain assemblies to reduce system energy and reach a stable situation spontaneously, for example, an energetically favorable micelle in water and a reverse micelle in organic medium.[1] On the basis of the micellar rule, many practical techniques have been developed in industry and scientific fields, for example, in the synthesis of nanoparticles including nanowires,[2] nanotubes,[3] nanorods,[4] spherical nanoparticles, etc.[5−29] Due to different physical properties caused by size effect compared with bulk materials, nanoparticles, considered as a latent material in nanoelectronics,[30] catalysis,[31] optics,[32] molecule sensors,[33] molecule recognition,[34] biosystems,[35] and other fields[36] have been one of the most fascinating fields recently. Herein, during the process of generating nanoparticles, for a micelle, one of the most important applications may be attributed to micellar solubilization. Micellar (reverse micellar) solubilization is commonly described that insoluble materials become soluble by incorporating them into the interior of the micelle (reverse micelle).[1] The inner core of reverse micelle or micelle, as a nanoreactor, has been a proven powerful tool in synthesizing nanoparticles because it can perform limitation of particle size and resistance of particles coalescence.[5−29]

In the past several decades, based on micellar solubilization, various strategies have been achieved in manufacturing nanoparticles. Noticeably, Brust and co-workers synthesized gold nanoparticles through a two-phase method that impelled the studies of gold nanoparticles greatly in 1994.[29] Recently, expanding the micellar solubilization to solid materials, the idea has been exploited in nanoparticles surface modification.[37−39] The protective surface of nanoparticles always determines solubility which in turn affects the applications of nanoparticles.[37] For example, hydrophobic metal nanoparticles possess an excellent ability to assemble ordered superlattice[40] and hydrophilic metal nanoparticles have predominant biocompatibility[35] so it is desirable and practical to modify the nanoparticle surface. On the basis of micellar-like solubilization, oil-soluble gold nanoparticles were transferred into aqueous solution with cetyltrimethylammonium bromide as the phase transfer agent.[37] Similarly, water-soluble semiconductors and other metal nanoparticles were prepared successfully.[38,39] Those foregoing attempts all involved using the hydrophobic nanoparticles stabilized by long alkyls as solubilized materials and wrapping the nanoparticles into a micellar-like core of secondary protective layers. Because no ligand exchange and chemical reaction happened to the metal core, in contrast with another main surface modification strategy of ligand exchange,[41] these methods had an evident advantage that the size and optical properties of nanoparticles were reserved, which rendered hydrophobic nanoparticles possible for application in a biosystem because only water-soluble nanoparticles possessed good biocompatibility. Meanwhile, because of the strong interaction of protective multilayers, those nanoparticles lost the original solubility after solubilization and could not be redispersed in organic solvent. That is to say, irreversible change happened to the solubility of those nanocrystals.

Here, based on the same idea, using PVP as a common polymer, we develop a protocol in which nanoparticles can show solublility in oil and water. Via the adsorption and desorption of polymer on the primary protective layer of hydrophobic metal nanoparticles driven by the minimum energy rule, the hydrophobic and hydrophilic gold nanoparticles can be transformed into each other by using hydrophobic gold nanoparticles capped by octadecylamine (ODA-gold) as primary materials. The primary ODA-gold nanoparticles only show good solubility in chloroform because the protective long alkyl chains lead to a great hydrophobic feature. However, under the effect of PVP,

* Address correspondence to this author. Phone: +86-21-64252214. Fax: +86-21-64252485. E-mail: jinmu@ecust.edu.cn.
† East China University of Science and Technology.
‡ Chinese Academy of Sciences.

10.1021/jp060892a CCC: $33.50
Published on Web 08/05/2006

the ODA-gold nanoparticles can dissolve in water and show almost the same optical and visible properties as those for ODA-gold in chloroform. Interestingly, when water is removed completely from hydrosol, the remaining gold nanoparticles can be redispersed in chloroform. As far as we know, gold nanoparticles possessing such a reversible soluble property only have two publications so far.[42,43] Meanwhile, robust size-controllable and water-soluble spherical assemblies, an active scientific field presently, considered as promising catalysts also can be generated easily through controlling conditions. If needed, the sphere nanostructure also can be converted into individual hydrophobic nanoparticles again. UV−vis spectroscopy, TEM, and FTIR are employed to observe the reversible process. The detailed investigation and thermodynamic interpretation are presented in the following.

Experimental Section

The size of ODA-gold nanoparticles can be tuned through controlling temperature and changing reaction solvent environment as described in previous reports. Gold nanoparticles stabilized by dodecanethiol (DDT-gold) with three sizes were prepared according to a similar Brust two-phase method at different temperatures.[29]

Synthesis of 5 nm ODA-Gold Nanoparticles. A typical synthesis procedure is the following: octadecylamine (0.4666 g, 0.0027 mol) was dissolved in 90 mL of chloroform, and then tetrachloroaurate chloroform solution (10 mL, 0.012 mol) was added to obtain a yellow solution. After ultrasonic treatment for about 3 h, the mixture changed from yellow to nearly colorless. Then sodium borohydride dissolved in ethanol (5 mL, 0.0013 mol) was added to reduce tetrachloroaurate under vigorous stirring and the colorless solution became aubergine quickly, which indicated gold nanoparticles had formed. After continued stirring for 12 h, most of the chloroform was removed through evaporation, and then 200 mL of ethanol was added to precipitate nanoparticles. The precipitation was washed several times to remove excess surfactants, and then dried at 54 °C for one night. The completely dried gold nanoparticles can be redissolved into chloroform.

Procedure of the Reversible Conversion of Hydrophobic ODA-Gold and PVP-ODA-Gold. As-prepared ODA-gold nanoparticles (0.012 mmol) were redispersed in chloroform (50 mL) and PVP (2 g, 0.018 mol) was added under stirring. Then a homogeneous colloid was obtained. Through rotary evaporation, chloroform solvent was dried completely and then water was added. The hydrosol was stirred for 12 h to solubilize completely. When the aqueous colloid was precipitated under centrifugal effect, and the obtained precipitation was ODA-gold coated with PVP (PVP-ODA-gold). The PVP-ODA-gold was redispersed into chloroform or water and the reclaimed precipitation from the organic colloid under centrifugal effect was ODA-gold (Re-ODA-gold).

Procedure for Preparing Hydrophilic Spherical Assembly. A typical synthesis proceeds as follows. Gold nanoparticles (0.0024 mmol) with different diameters and functional agents were redispersed in chloroform (50 mL) containing different amounts of PVP (4 g, 0.036 mol; 1.33 g, 0.012 mol; 0.27 g, 0.0024 mol; 0.027 g, 0.00018 mol; 0.0027 g, 0.000018 mol; 0 g, 0 mol). At room temperature, the chloroform was dried fully and deionized water (20 mL) was added. To coat completely, the aqueous solution was stirred for 12 h. Then the collected precipitate from the above five sols was washed with water to remove excess PVP (16 000 rpm).

Characterization. Pure ODA, as-prepared ODA-gold, and Re-ODA-gold were dispersed in chloroform then the solutions were dropped on calcium fluoride plates to dry the solvent. The completely dried calcium fluoride plates were used as FTIR samples. For pure PVP and individual PVP-ODA-gold samples, the washed precipitation was redispersed in water, and then the hydrosols were placed on calcium fluoride plates. The plates were dried at 54 °C completely and then measured with FTIR.

For TEM samples, a drop of the chloroform colloid solution from as-prepared ODA-gold and Re-ODA-gold was placed on carbon-coated copper grids. For hydrophilic spherical assemblies and PVP-ODA-gold, the hydrosols were used. Before observation, it was necessary for all TEM samples to dry at 54 °C for 2 h.

SCHEME 1: Reversible Procedure between ODA-Gold and PVP-ODA-Gold

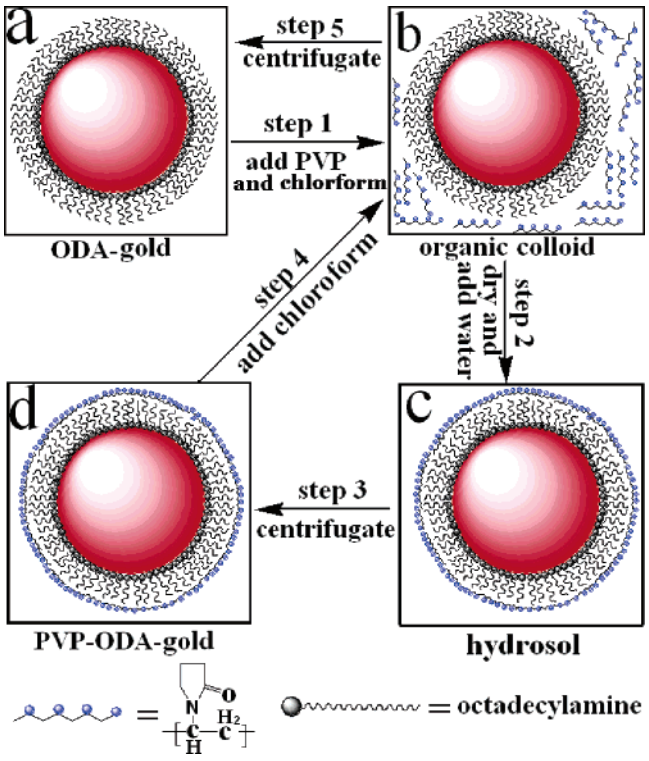

Results and Discussion

Reversible Conversion between Hydrophobic Gold Nanoparticles and Hydrophilic Nanostructures. Scheme 1 presents a detailed process of the reversible conversion involving five main steps. Primary gold nanoparticles functioned by ODA organic monolayer (Scheme 1a) cannot dissolve in water alone because the strong hydrophobic character of alkyl chains leads to great interface energy. However, upon mixing PVP with ODA-gold in chloroform (step 1), drying with chloroform completely, and adding water, induced by the reduction of interfacial energy, ODA-gold will be encapsulated inside the core of PVP-like-micelle to form hydrophilic PVP-ODA-gold (Scheme 1c) under the effect of the pyrrole loop (step 2). Expanding conventional micellar solubilization of oil in micelle to our experiment this can be understood easily if the ODA-gold is considered as an oil drop. Under the centrifugal effect, the deposition from hydrosol is PVP-ODA-gold (Scheme 1d) after washing with water to remove excess PVP (step 3). Both in chloroform and in water, PVP-ODA-gold nanoparticles show good redispersed ability. When PVP-ODA-gold nanoparticles are redispersed in chloroform and the reducing trend of interfacial energy affects the system again, the PVP molecules

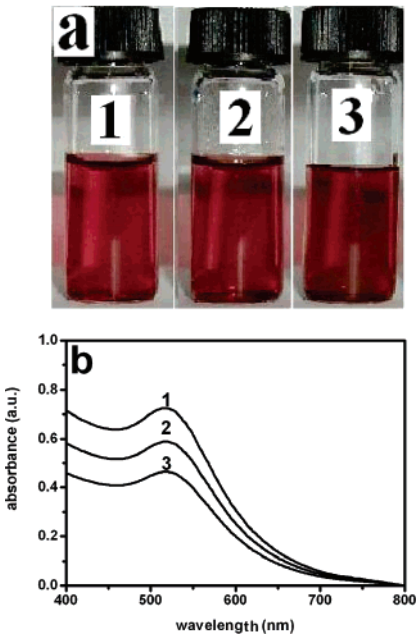

Figure 1. (a) Photographs of as-prepared ODA-gold in chloroform (tube 1), PVP-ODA-gold in water (tube 2), and Re-ODA-gold in chloroform (tube 3); (b) UV−vis spectra of tube 1 (curve 1), tube 2 (curve 2), and tube 3 (curve 3).

fall off from the PVP-ODA-gold nanoparticles and the ODA-gold nanoparticles are released and surrounded by chloroform again (step 4). When the organic colloid is exposed to centrifugation and washed many times the reclaimed precipitate is Re-ODA-gold (step 5).

To investigate the reversible procedure in which PVP and ODA-gold interact, visible color, TEM, UV−vis, and FTIR are used to monitor experiments. ODA-gold (tube 1), PVP-ODA-gold (tube 2), and the Re-ODA-gold nanoparticles (tube 3) after a cycle exhibit the same visible and emission colors as shown in the optical micrographs (Figure 1a). Further, sensitive UV−vis spectroscopy is used to determine the difference among three samples, as shown in Figure 1B. On the basis of Mie theory,[43] the particle size and interparticle distance play an important role in the absorbance and wavelength of the band and optical color. For example, the individual 4.6 nm gold nanoparticles coated by an organic monolayer have a typical absorption peak at 525 nm, however, the spherical assemblies of the nanoparticles possess an obvious absorption band at about 700 nm.[44,45] In our experiment, we find that there is no difference in the position of the absorption bands for the three nanoparticles (curve 1 for ODA-gold, curve 2 for PVP-ODA-gold, and curve 3 for Re-ODA-gold) which provides definite evidence that the transformed PVP-ODA-gold and regained ODA-gold can maintain their optical properties and original size. The results can provide the opportunity for the hydrophobic ODA-gold nanoparticles to be used in a biosystem because PVP is nontoxic and in turn PVP-ODA-gold is biocompatible.

Hydrophobic metal, semiconductor, or metal oxide nanoparticle colloids can form ordered superlattice structures on substrate or interface under the pinning effect and the entropy-driven ordering tendency upon solvent evaporation.[40] However, for water-soluble nanoparticles, because solvent cannot provide a suitable evaporating rate and interactions between particles, the large-scale area assembly with ordered feature is hard to obtain. Here, the as-prepared 5 nm ODA-gold nanoparticles are dispersed in chloroform and dropped on a copper grid coated by carbon, generating a local superlattice after solvent evaporated, shown in Figure 2a. Although PVP-ODA-gold in water is also kept dispersed, but ordered structure is still scarce, as shown in Figure 2b, whereas the PVP-ODA-gold is redispersed in chloroform and undergoes centrifugation, the precipitate redispersed in chloroform can form an ordered superlattice (Figure 2c), which indicates the precipitate is ODA-gold and PVP desorbs from PVP-ODA-gold in organic solvent indirectly. It is also indicative that ODA-gold nanoparticles can be used both in biosystem possibility and assembly, using ODA-gold as raw material by simply varying the protective layers. It is also necessary to note that ordered two-dimensional assemblies of hydrophobic nanoparticles have attained increasing interest because of their potential application in electronics and optics.[40]

To further shed light on the interaction mechanism of how PVP molecules interact with ODA-gold in different medium, FTIR is used as a detecting tool to observe gold nanoparticles at different stages depicted in Scheme 1. The results from 5 nm as-prepared ODA-gold, pure ODA, and Re-ODA-gold are shown in Figure 3a. The results obtained from pure PVP and PVP-ODA-gold are illustrated in Figure 3b. In Figure 3a, the three curves all possess similar absorption below 3000 cm^{-1}. Above 3000 cm^{-1}, curves 1 and 3 lack the typical absorption of N−H at 3400 cm^{-1} compared with curve 2, which is due to the formation of the Au−N covalent bond and the disappearance of the N−H covalent bond. The result is consistent with another report.[46] In Figure 3b, there are the same absorption bands corresponding to a typical absorption of C═O vibration at 1640 cm^{-1}, which suggests a safe conclusion that a secondary protective layer or PVP-ODA-gold is formed in water. No difference between two curves in Figure 3b is ascribed to no direct coordination between PVP and ODA-gold. FTIR results,

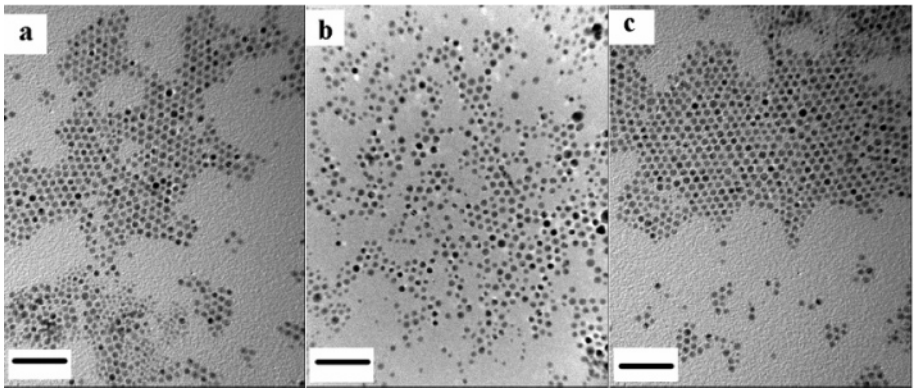

Figure 2. Representative TEM pictures of (a) local superlattice from as-prepared ODA-gold; (b) water-soluble PVP-ODA-gold; and (c) ordered assembly from ODA-gold after reversible cycle. Scale bar: 50 nm.

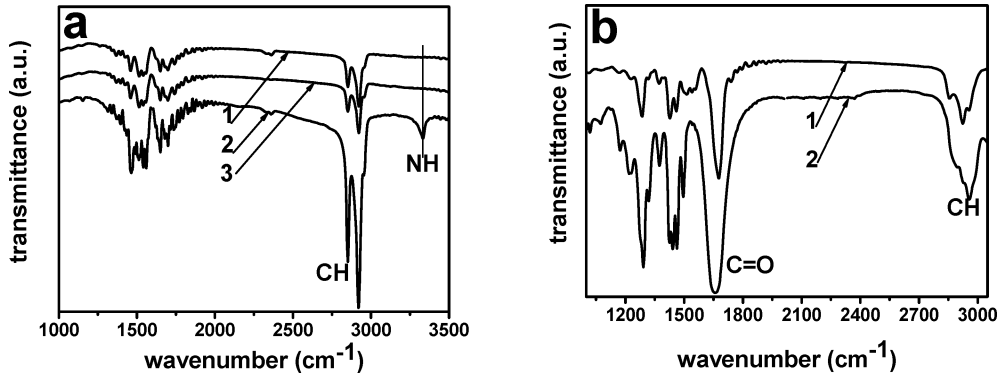

Figure 3. (a) FTIR spectra of as-prepared ODA-gold (curve 1), pure ODA (curve 2), and Re-ODA-gold (curve 3); (b) FTIR spectra of pure PVP (curve 1) and PVP-ODA-gold (curve 2).

SCHEME 2: Interfacial Competition Induced by Reduction of Interfacial Energy in Different Solvent Medium

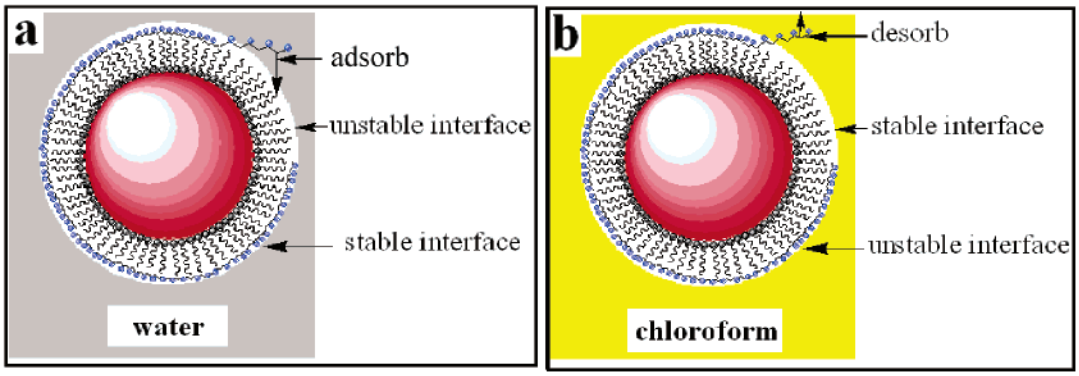

in agreement with the above TEM, optical, and UV−vis investigation, cooperate to provide the realization of a reversible procedure.

Thermodynamic Interpretation. According to the minimum energy rule, the process can be explained thermodynamically. For a system, the G can be described as

$$G = VP + E - ST \tag{1}$$

where T, P, V, G, E, and S represent termperature, pressure, volume, Gibbs free energy, interfacial energy, and entropy, respectively. The differential equation of (1) is

$$\mathrm{d}G = P\,\mathrm{d}V + V\,\mathrm{d}P + \mathrm{d}(A\sigma) - S\,\mathrm{d}T - T\,\mathrm{d}S \tag{2}$$

in which the interface area and interfacial tension are represented by A and σ, respectively. When the system temperature, bulk, pressure, and the component are kept constant, eq 2 can be simplified as

$$\mathrm{d}G = \mathrm{d}(\sigma A) \tag{3}$$

Equation 3 illustrates that the change of free energy is equal to the change of the interfacial energy. In a colloid system, the colloid particle diameter determines the surface area directly, so the system stability is in turn determined by the colloid unit diameter and the difference of interfacial tension. If the size of the colloid unit is monosized r and the number of colloid units is m, eq 3 can be rewritten as

$$\mathrm{d}G = 8m\pi\sigma\,\mathrm{d}r + mA\,\mathrm{d}\sigma + A\sigma\,\mathrm{d}m \tag{4}$$

where r is equal to the mean diameter of particles. The equation shows that dG is only dependent on the change of the particle size and interfacial tension. For dispersed nanoparticles, although the outer polymer layer can increase the size of nanoparticles, we cannot observe the size change of nanoparticles based on TEM and UV−vis results because the polymer layer is very thin compared with the diameter of nanoparticles. So eq 4 can be reduced.

$$\mathrm{d}G = mA\,\mathrm{d}\sigma \tag{5}$$

When two phases are mixed, the initially formed interfaces are not favored thermodynamically and replacement of the interface is aroused by the interfacial competition. Finally, the interface with the lowest interfacial tension that is satisfied thermodynamically will dominate the system and determine the structure of the mixed phase.

During the reversible conversion between PVP-ODA-gold and ODA-gold, when the PVP and ODA-gold are dispersed in water, because great interfacial tension exists at the interface made by the long alkyl chains layer of ODA-gold and water (unstable interface designated in Scheme 2a), such great interfacial energy makes the system fall into a pretty unstable situation. Subsequently, an interfacial replacement happens to the colloid system spontaneously. Finally, the alkyl chains of PVP molecules coat the octadecyl chain monolayer of ODA-gold and the new interface (the interface between the secondary layer of the hydrophilic pyrrolidone loop and water is designated by the stable interface shown in Scheme 2a) with lower interfacial tension replaces the ODA-gold/water interface to lower interfacial energy. On the basis of eq 5, it is understood lightly that the formation of a new interface is really beneficial to the stability of the system. However, when PVP-ODA-gold is redispersed in chloroform, in contrast with the interface between the octadecyl chain layer and chloroform, the interface between the pyrrole loop layer and chloroform possesses higher interfacial tension and energy, so the system is unstable and PVP molecules fall off from ODA-gold to release ODA-gold and

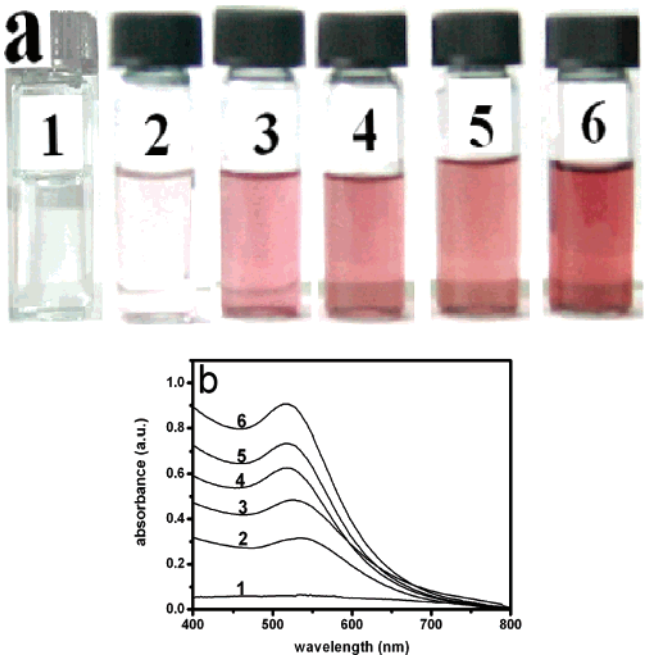

Figure 4. (a) Optical images of gold sols from different molar ratios of PVP/ODA-gold, 0 (bottle 1), 0.001 (bottle 2), 0.01 (bottle 3), 0.1 (bottle 4), 0.5 (bottle 5), 1.5 (bottle 6); (b) UV−vis spectra, curve 1, curve 2, curve 3, curve 4, curve 5, and curve 6 responsible for sols bottle 1, bottle 2, bottle 3, bottle 4, bottle 5, and bottle 6, respectively.

the ODA-gold/chloroform interface having low energy (stable interface shown in Scheme 2b) replaces the pyrrolidone-loop/chloroform interface with relative high energy (unstable interface shown in Scheme 2b).

Formation of Sphere Nanostructure. We initially attempted to investigate the effect of the amount of PVP on hydrophilic PVP-ODA-gold, so we adjusted the ratio of PVP/ODA-gold. The UV−vis absorbance and optical color of PVP/ODA-gold are a function of the mole ratio, as shown in Figure 4. On decreasing the mole ratio of PVP/ODA-gold, the UV−vis absorbance shows a red shift and the optical color weakens, which is indicative of the formation of aggregates with larger size based on Mie theory.[44] Besides, when the mole ratio of PVP/ODA-gold is 0, no gold nanoparticles enter the water solution, which provides sound evidence that ODA-gold is transferred into hydrophilic nanoparticles under the effect of PVP. The hydrosols are exposed to centrifugation and the precipitation is further determined with use of TEM and the results (Figure 5) are consistent with the UV−vis results. Interestingly, the morphology of aggregates is almost a sphere where nanoparticles can be distinguished clearly. On increasing the mole ratio of PVP/ODA-gold, the size of aggregation of nanoparticles shows a size decreasing trend and the dispersed PVP-ODA-gold nanoparticles are obtained when the mole ratio of PVP/ODA-gold is kept over 1.5. Moreover, increasing the mole ratio of PVP/ODA-gold will make the sedimentation of the sphere nanostructure harder, which indicates that higher PVP/ODA-gold leads to the formation of the sphere nanostructure with smaller size.

Many researchers report that sphere nanostructures possess unique catalyst application. Recently, sphere nanostructure aggregates have attained increasing interest and different protocols, such as mediate-template, molecular hydrogen bond interaction, and covalent interaction, have been demonstrated to guide the sphere formation with use of nanoparticles as building block.[45,47−54] In our experiment, unlike previous reports, we employ the micellar-like solubilization to construct spherical aggregates using different metal nanoparticles with various sizes and capping agents. The results show the method can be viewed as a general route to assemble nanoparticles into sphere nanostructures. Three ODA-gold and three DDT-gold nanoparticles of different size are used to form spherical aggregates. The results for 2.5 nm DDT-gold are shown in Figure 6 (for other five nanoparticles and relative results see the Supporting Information). The DDT-gold (Figure 6a) and size distribution (Figure 6b) indicate that the DDT-gold has a narrow size scope and monosized feature. For spherical aggregates, a low-

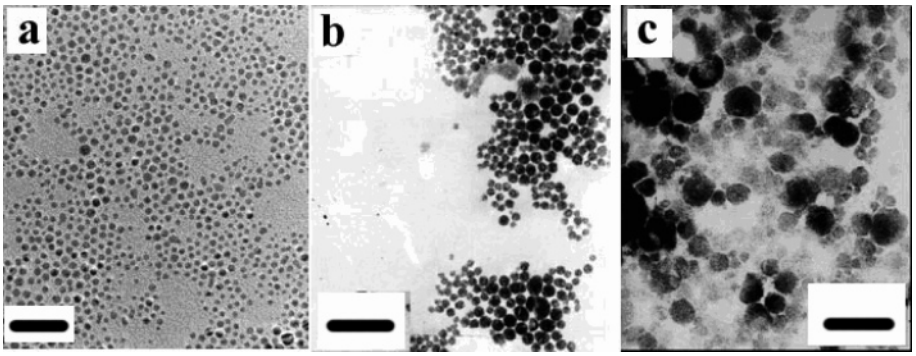

Figure 5. Typical TEM images of samples from PVP/gold molar ratios of (a) 1.5, scale bar 45 nm; (b) 0.5, scale bar: 470 nm; and (c) 0.01, scale bar: 470 nm.

SCHEME 3: Sphere Formation through Unstable Interfacial Combination

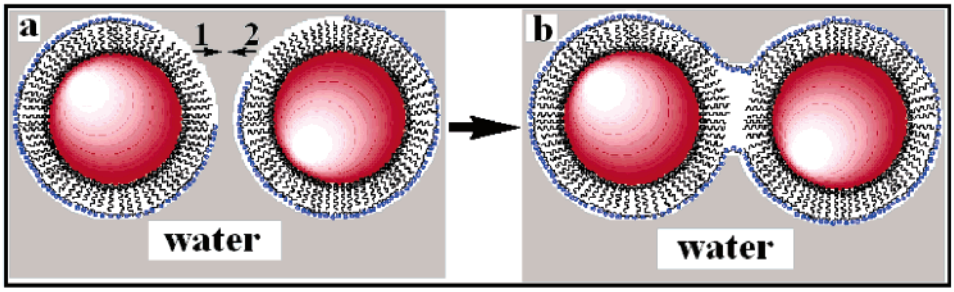

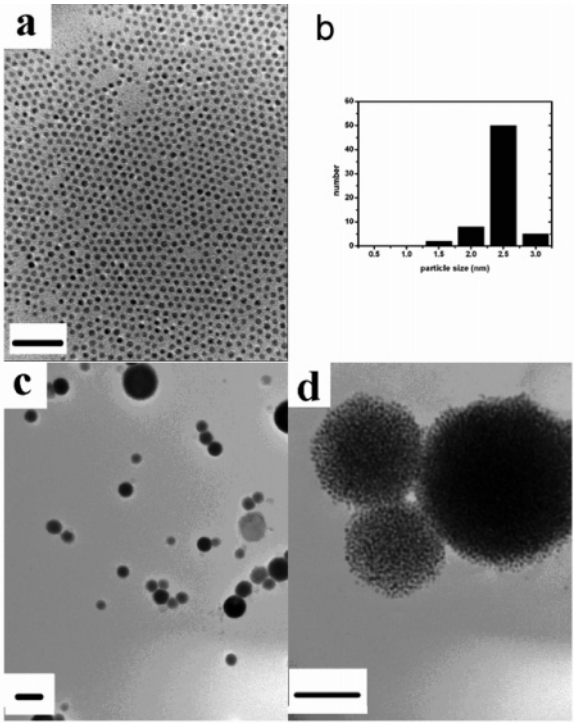

Figure 6. (a) Representative TEM of 2.5 nm monodispersed DDT-gold, scale bar: 20 nm; (b) size distribution of DDT-gold; (c) TEM of water-dispersed sphere nanostructures, scale bar: 200 nm; and (d) magnified image (c), scale bar: 50 nm.

resolution TEM picture (Figure 6c) suggests that many sphere nanostructures are obtained and a clear sphere nanostructure can be distinguished from high-resolution TEM (Figure 6d). The sphere nanostructures possess a sponge-like structure where individual particles are observed distinctly. Moreover, redispersed experiment shows the sphere nanostructure can be conversed into dispersed ODA-gold nanoparticles again through redispersing it in chloroform and centrifugating like PVP-ODA-gold.

For spherical aggregates, it is reasonable to analyze interfacial energy by using eq 4, instead of eq 5, due to the distinct change of size and decrease of the number of colloid units. As the mole ratio of PVP/ODA-gold is decreased, obviously it is hard for PVP molecules to coat ODA-gold nanoparticles completely and partial octadecyl chains have to be exposed to water, so the system becomes unstable because the water/ODA interface results in high interfacial energy. That is to say, interfacial replacement does not have the ability to give rise to the system with the lowest energy. It is well-known that, compared with individual particles, the spherical assemblies of particles with larger diameter possess low energy and in turn do well to reduce interfacial energy because of small interfacial area. So the octadecyl chains without the PVP layer (interfaces of the **1** and **2** depicted in Scheme 3a) will come close and contact each other. According to eq 4, although the diameter r of assembly blocks increases, the total energy decreases because of considerable reduction of the unit number m. Finally, the ODA/water interface disappears and the system becomes relatively stable because of reduction of interfacial energy (shown in Scheme 3b). When more ODA-gold nanoparticles possessing unstable structure exist, spherical assemblies form. Obviously, the mole ratio of PVP/ODA-gold determines the coat layer area of PVP on ODA-gold, which in turn determines the number of ODA-gold nanoparticles in assemblies, so size-controllable sphere structures can be obtained through adjusting the mole ratio of PVP/ODA-gold.

Conclusions

In summary, we have demonstrated that based on micellar-like solubilization theory, hydrophobic ODA-gold and hydrophilic PVP-ODA-gold nanoparticles can be transformed reversibly by using ODA-gold as the initial material through adsorption and desorption of PVP molecules on ODA-gold nanoparticles. Moreover, during the transformation, the physical properties (optical, electronic, etc.) and size can be maintained well because chemical reaction and ligand exchange are avoided. Additionally, size-controllable spherical assemblies of gold nanoparticles with various diameter and capping agents can be gained simply through modulating the polymer/gold ratio. We suppose that the mechanism and protocol presented here can be extended to other metal nanoparticle solubility modification and assembly according to practical need.

Acknowledgment. This work was supported by the National Science Foundation of China (90207026). We thank Prof. Shujie Li for use of FTIR and Dr. Xun Kuang for assistance in TEM measurement and analysis.

Supporting Information Available: Detailed experiments for the synthesis of 0.8, 3.2, and 5.3 nm ODA-gold and 1.2, 2.5, and 3.3 nm DDT-gold. This material is available free of charge via the Internet at http://pubs.acs.org.

References and Notes

(1) (a) Melo, E.; Freitas, A. A.; Yihwa, C.; Quina, F. H. *Langmuir* **2001**, *17*, 7980. (b) Orihara, Y.; Matsumura, A.; Saito, Y.; Ogawa, N.; Saji, T.; Yamaguchi, A.; Sakai, H.; Abe, M. *Langmuir* **2001**, *17*, 6072. (c) Choucair, A.; Eisenberg, A. *J. Am. Chem. Soc.* **2003**, *125*, 11993.

(2) (a) Xu, S.; Zhou, H.; Xu, J.; Li, Y. *Langmuir* **2002**, *18*, 10503. (b) Shi, H.; Qi, L.; Ma, J.; Cheng, H. *J. Am. Chem. Soc.* **2003**, *125*, 3450. (c) Niu, H.; Zhang, L.; Gao, M.; Chen, Y. *Langmuir* **2005**, *21*, 4205. (d) Jiang, X.; Xie, Y.; Lu, J.; Zhu, L.; He, W.; Qian, Y. *Chem. Mater.* **2001**, *13*, 1213. (e) Sun, Y.; Gates, B.; Mayers, B.; Xia, Y. *Nano Lett.* **2002**, *2*, 165.

(3) (a) Ma, Y.; Qi, L.; Ma, J.; Cheng, H. *Adv. Mater.* **2004**, *16*, 1023. (b) Harada, M.; Adachi, M. *Adv. Mater.* **2000**, *12*, 839. (c) Ni, C.; Hassan, P. A.; Kaler, E. W. *Langmuir* **2005**, *21*, 3334. (d) Sau, T. K.; Murphy, C. J. *J. Am. Chem. Soc.* **2004**, *126*, 8648.

(4) (a) Jana, N. R.; Gearheart, L.; Murphy, C. J. *J. Phys. Chem. B* **2001**, *105*, 4065. (b) Gou, L.; Murphy, C. J. *Chem. Mater.* **2005**, *17*, 3668. (c) Gao, J.; Bender, C. M.; Murphy, C. J. *Langmuir* **2003**, *19*, 9065.

(5) Lala, N.; Lalbegi, S. P.; Adyanthaya, S. D.; Sastry, M. *Langmuir* **2001**, *17*, 3766.

(6) Hussain, I.; Brust, M.; Papworth, A. J.; Cooper, A. I. *Langmuir* **2003**, *19*, 4831.

(7) Zhang, H.; Hussain, I.; Brust, M.; Cooper, A. I. *Adv. Mater.* **2004**, *16*, 27.

(8) Hassenkam, T.; Nørgaard, K.; Iversen, L.; Kiely, C. J.; Brust, M.; Bjørnholm, T. *Adv. Mater.* **2002**, *14*, 1126.

(9) Jana, N. R.; Gearheart, L.; Murphy, C. J. *Langmuir* **2001**, *17*, 6782.

(10) Sau, T. K.; Murphy, C. J. *Langmuir* **2005**, *21*, 2923.

(11) Jana, N. R.; Gearheart, L.; Murphy, C. J. *Chem. Mater.* **2001**, *13*, 2313.

(12) Murphy, C. J.; Sau, T. K.; Gole, A. M.; Orendorff, C. J.; Gao, J.; Gou, L.; Hunyadi, S. E.; Li, T. *J. Phys. Chem. B* **2005**, *109*, 13857.

(13) Toshima, N.; Shiraishi, Y.; Teranishi, T.; Miyake, M.; Tominaga, T.; Watanabe, H.; Brijoux, W.; Bönnemann, H.; Schmid, G. *Appl. Organomet. Chem.* **2001**, *15*, 178.

(14) Embden, V. J.; Mulvaney, P. *Langmuir* **2005**, *21*, 10226.

(15) Mulvaney, P.; Giersig, M.; Ung, T.; Liz-Marzán, L. M. *Adv. Mater.* **1997**, *9*, 570.

(16) Gittins, D. I.; Caruso, F. *ChemPhysChem* **2002**, *3*, 110.

(17) Gittins, D. I.; Caruso, F. *Angew. Chem., Int. Ed.* **2001**, *40*, 3001.

(18) Mayya, K. S.; Caruso, F. *Langmuir* **2003**, *19*, 6987.

(19) Garcia-Martinez, J. C.; Scott, R. W. J.; Crooks, R. M. *J. Am. Chem. Soc.* **2003**, *125*, 11190.

(20) Hiramatsu, H.; Osterloh, F. E. *Chem. Mater.* **2004**, *16*, 2509.

(21) Song, H.; Kim, F.; Connor, S.; Somorjai, G. A.; Yang, P. *J. Phys. Chem. B* **2005**, *109*, 188.

(22) Lu, Y.; Yin, Y.; Li, Z.-Y.; Xia, Y. *Nano Lett.* **2002**, *2*, 785.

(23) Kim, F.; Connor, S.; Song, H.; Kuykendall, T.; Yang, P. *Angew. Chem., Int. Ed.* **2004**, *43*, 3673.

(24) Prasad, B. L. V.; Stoeva, S. I.; Sorensen, C. M.; Klabunde, K. J. *Chem. Mater.* **2003**, *15*, 935.
(25) Lin, X. M.; Jaeger, H. M.; Sorensen, C. M.; Klabunde, K. J. *J. Phys. Chem. B* **2001**, *105*, 3353.
(26) Cheng, W.; Wang, E.*J. Phys. Chem. B* **2004**, *108*, 24.
(27) Cheng, W.; Dong, S.; Wang, E. *J. Phys. Chem. B* **2005**, *109*, 9213.
(28) Chen, X. Y.; Li, J. R.; Jiang, L. *Nanotechnology* **1999**, *11*, 108.
(29) (a) Brust, M.; Walker, M.; Bethell, D.; Schiffrin, D. J.; Whyman, R. *J. Chem. Soc., Chem. Commun.* **1994**, 801. (b) Brust, M.; Kiely, C. J. *Colloids Surf. A* **2002**, *202*, 175. (c) Brust, M.; Fink, J.; Bethell, D.; Schiffrin, D.; Kiely, C. J. *J. Chem. Soc., Chem. Commun.* **1995**, 1655.
(30) (a) Li, Y.; Wu, Y.; Ong, B. S. *J. Am. Chem. Soc.* **2005**, *127*, 3266. (b) Paul, S.; Pearson, C.; Molloy, A.; Cousins, M. A.; Green, M.; Kolliopoulou, S.; Dimitrakis, P.; Normand, P.; Tsoukalas, D.; Petty, M. C. *Nano Lett.* **2003**, *3*, 533.
(31) (a) Yan, W.; Chen, B.; Mahurin, S. M.; Schwartz, V.; Mullins, D. R.; Lupini, A. R.; Pennycook, S. J.; Dai, S.; Overbury, S. H. *J. Phys. Chem. B* **2005**, *109*, 10676. (b) Noskov, J. K.; Lopez, N.; Remediakis, I. N. *Angew. Chem., Int. Ed.* **2005**, *44*, 1824.
(32) (a) Schmid, G.; Corain, B. *Eur. J. Inorg. Chem.* **2003**, 3081. (b) Larsson, M.; Lu, J.; Lindgren, J. *J. Raman Spectrosc.* **2004**, *35*, 826. (c) Kneipp, J.; Kneipp, H.; Rice, W. L.; Kneipp, K. *Anal. Chem.* **2005**, *77*, 2381. (d) Landes, C.; Burda, C.; Braun, M.; El-Sayed, M. A. *J. Phys. Chem. B* **2001**, *105*, 2981.
(33) (a) Tao, A.; Kim, F.; Hess, C.; Goldberger, J.; He, R.; Sun, Y.; Xia, Y.; Yang, P. *Nano Lett.* **2003**, *3*, 1229. (b) Maiti, A.; Rodriguez, J. A.; Law, M.; Kung, P.; McKinney, J. R.; Yang, P. *Nano Lett.* **2003**, *3*, 1025.
(34) (a) Raschke, G.; Kowarik, S.; Franzl, T.; Sonnichsen, C.; Klar, T. A.; Feldmann, J.; Nichtl, A.; Kurzinger, K. *Nano Lett.* **2003**, *3*, 935. (b) Naka, K.; Itoh, H.; Chujo, Y. *Langmuir* **2003**, *19*, 5496. (c) Wang, Z.; Levy, R.; Fernig, D. G.; Brust, M. *Bioconj. Chem.* **2005**, *16*, 497.
(35) (a) Taton, T. A.; Mirkin, C. A.; Letsinger, R. L. *Science* **2000**, *289*, 1757. (b) Storhoff, J. J.; Lucas, A. D.; Garimella, V.; Bao, Y. P.; Müller, U. R. *Nat. Biotechnol.* **2004**, *22*, 883. (c) Nazzal, A. Y.; Qu, L.; Peng, X.; Xiao, M. *Nano Lett.* **2003**, *3*, 819. (d) Grancharov, S. G.; Zeng, H.; Sun, S.; Wang, S. X.; O'Brien, S.; Murray, C. B.; Kirtley, J. R.; Held, G. A. *J. Phys. Chem. B* **2005**, *109*, 13030.
(36) Daniel, M.-C.; Astruc, D. *Chem. Rev.* **2004**, *104*, 293.
(37) (a) Swami, A.; Kumar, A.; Sastry, M. S. *Langmuir* **2003**, *19*, 1168. (b) Qu, L.; Peng, X. *J. Am. Chem. Soc.* **2002**, *124*, 2049. (c) Li, Y.; Zhang, Q.; Nurmikko, A. V.; Sun, S. *Nano Lett.* **2005**, *5*, 1689.
(38) (a) Fan, H. Y.; Chen, Z.; Brinker, C. J.; Clawson, J.; Alam, T. *J. Am. Chem. Soc.* **2005**, *127*, 13746. (b) Fan, H.; Leve, E. W.; Scullin, C.; Gabaldon, J.; Tallant, D.; Bunge, S.; Boyle, T.; Wilson, M. C.; Brinker, C. J. *Nano Lett.* **2005**, *5*, 645. (c) Fan, H. Y.; Yang, K.; Boye, D. M.; Sigmon, T.; Malloy, K. J.; Xu, H. F.; Lopez, G. P.; Brinker, C. J. *Science* **2004**, *304*, 567.
(39) Pellegrino, T.; Manna, L.; Kudera, S.; Liedl, T.; Koktysh, D.; Rogach, A. L.; Keller, S.; Radler, J.; Natile, G.; Parak, W. J. *Nano Lett.* **2004**, *4*, 703.
(40) (a) Santhanam, V.; Liu, J.; Agarwal, R.; Andres, R. P. *Langmuir* **2003**, *19*, 7881. (b) Petroski, J. M.; Green, T. C.; El-Sayed, M. A. *J. Phys. Chem. A* **2001**, *105*, 5542. (c) Kiely, C. J.; Fink, J.; Brust, M.; Bethell, D.; Schiffrin, D. J. *Nature* **1998**, *396*, 444. (d) Motte, L.; Lacaze, E.; Maillard, M.; Pileni, M. P. *Langmuir* **2000**, *16*, 3803. (e) Murray, C. B.; Kagan, C. R.; Bawendi, M. G. *Science* **1997**, *270*, 1335.
(41) (a) Yang, J.; Lee, J.; Chen, L. X.; Too, H.-P. *J. Phys. Chem. B* **2005**, *109*, 5468. (b) Yang, J.; Deivaraj, T. C.; Too, H.-P.; Lee, J. *J. Phys. Chem. B* **2004**, *108*, 2181. (c) Sarathy, K. V.; Raina, G.; Yadav, R. T.; Kulkarni, G. U.; Rao, C. N. *J. Phys. Chem. B* **1997**, *101*, 9876. (d) Ackerson, C. J.; Jadzinsky, P. D.; Kornberg, R. D. *J. Am. Chem. Soc.* **2005**, *127*, 6550.
(42) Duan, H.; Kuang, M.; Wang, D.; Kurth, D. G.; Möhwald, H. *Angew. Chem., Int. Ed.* **2005**, *44*, 1717.
(43) Prasad, B. L. V.; Arumugam, S. K.; Bala, T.; Sastry, M. *Langmuir* **2005**, *21*, 822.
(44) (a) Link, S.; El-Sayed, M. A. *Int. Rev. Phys. Chem.* **2000**, *19*, 409. (b) Papavassiliou, G. C. *Prog. Solid State Chem.* **1979**, *12*, 185.
(45) Lim, I.-I. S.; Maye, M. M.; Luo, J.; Zhong, C. J. *J. Phys. Chem. B* **2005**, *109*, 2578.
(46) Kumar, A.; Mandal, S.; Selvakannan, P. R.; Pasricha, R.; Mandale, A. B.; Sastry, M. *Langmuir* **2003**, *19*, 6277.
(47) (a) Maye, M. M.; Chun, S. C.; Han, L.; Rabinovich, D.; Zhong, C.-J. *J. Am. Chem. Soc.* **2002**, *124*, 4958. (b) Maye, M. M.; Luo, J.; Lim, I.-I. S.; Han, L.; Kariuki, N. N.; Rabinovich, D.; Liu, T. B.; Zhong, C. J. *J. Am. Chem. Soc.* **2003**, *125*, 9906. (c) Maye, M. M.; Lim, I.-I. S.; Luo, J.; Rab, Z.; Rabinovich, D.; Liu, T.; Zhong, C. J. *J. Am. Chem. Soc.* **2005**, *127*, 1519.
(48) Zhong, Z.; Subramanian, A. S.; Highfield, J.; Carpenter, K.; Gedanken, A. *Chem. Eur. J.* **2005**, *11*, 1473l.
(49) Boal, A. K.; Ilhan, F.; DeRouchey, J. E.; Thurn-Albrecht, T.; Russell, T. P.; Rotello, V. M. *Nature* **2000**, *404*, 746.
(50) Vidoni, O.; Philippot, K.; Amiens, C.; Chaudret, B.; Balmes, O.; Malm, J.; Bovin, J.-O.; Senocq, F.; Casanove, M.-J. *Angew. Chem., Int. Ed.* **1999**, *38*, 3736.
(51) Pelzer, K.; Vidoni, O.; Philippot, K.; Chaudret, B.; Collière, V. *Adv. Funct. Mater.* **2003**, *13*, 118.
(52) Ewers, T. D.; Sra, A. K.; Norris, B. C.; Cable, R. E.; Cheng, C.-H.; Shantz, D. F.; Schaak, R. E. *Chem. Mater.* **2005**, *17*, 514.
(53) Jin, J.; Iyoda, T.; Cao, C.; Song, Y.; Jiang, L.; Li, T.; Zhu, D. *Angew. Chem., Int. Ed.* **2001**, *40*, 2135.
(54) Song, Y.; Yang, Y.; Medforth, C. J.; Pereira, E.; Singh, A. K.; Xu, H.; Jiang, Y.; Brinker, C. J.; van Swol, F.; Shelnutt, J. A. *J. Am. Chem. Soc.* **2004**, *126*, 635.